External cavity diode laser-based detection of trace gases with NICE-OHMS using current modulation

R. Centeno,[1] J. Mandon,[1] S. M. Cristescu,[1] O. Axner,[2] and F. J. M. Harren[1,*]

[1]*Life Science Trace Gas Facility, Radboud University Nijmegen, P.O. Box 9010, NL-6500 GL, The Netherlands*
[2]*Department of Physics, Umeå University, SE-901 87 Umeå, Sweden*
[*]*f.harren@science.ru.nl*

Abstract: We combine an external cavity diode laser with noise-immune cavity-enhanced optical heterodyne molecular spectroscopy (NICE-OHMS) using current modulation. With a finesse of 1600, we demonstrate noise equivalent absorption sensitivities of 4.1 x 10^{-10} cm^{-1} $Hz^{-1/2}$, resulting in sub-ppbv detection limits for Doppler-broadened transitions of CH_4 at 6132.3 cm^{-1}, C_2H_2 at 6578.5 cm^{-1} and HCN at 6541.7 cm^{-1}. The system is used for hydrogen cyanide detection from sweet almonds.

OCIS codes: (300.6340) Spectroscopy, infrared; (300.6360) Spectroscopy, laser; (300.6380) Spectroscopy, modulation; (140.4780) Optical resonators; (140.2020) Diode lasers; (140.3425) Laser stabilization.

References and links

1. G. Bjorklund, M. Levenson, W. Lenth, and C. Ortiz, "Frequency modulation (FM) spectroscopy," Appl. Phys. B **32**(3), 145–152 (1983).
2. J. Ye, L.-S. Ma, and J. L. Hall, "Ultrasensitive detections in atomic and molecular physics: demonstration in molecular overtone spectroscopy," J. Opt. Soc. Am. B **15**(1), 6–15 (1998).
3. A. Foltynowicz, W. Ma, and O. Axner, "Characterization of fiber-laser-based sub-Doppler NICE-OHMS for quantitative trace gas detection," Opt. Express **16**(19), 14689–14702 (2008).
4. L. Gianfrani, R. W. Fox, and L. Hollberg, "Cavity-enhanced absorption spectroscopy of molecular oxygen," J. Opt. Soc. Am. B **16**(12), 2247–2254 (1999).
5. N. J. van Leeuwen and A. C. Wilson, "Measurement of pressure-broadened, ultraweak transitions with noise-immune cavity-enhanced optical heterodyne molecular spectroscopy," J. Opt. Soc. Am. B **21**(10), 1713–1721 (2004).
6. C. L. Bell, G. Hancock, R. Peverall, G. A. Ritchie, J. H. van Helden, and N. J. van Leeuwen, "Characterization of an external cavity diode laser based ring cavity NICE-OHMS system," Opt. Express **17**(12), 9834–9839 (2009).
7. M. W. Porambo, B. M. Siller, J. M. Pearson, and B. J. McCall, "Broadly tunable mid-infrared noise-immune cavity-enhanced optical heterodyne molecular spectrometer," Opt. Lett. **37**(21), 4422–4424 (2012).
8. K. N. Crabtree, J. N. Hodges, B. M. Siller, A. J. Perry, J. E. Kelly, P. A. Jenkins II, and B. J. McCall, "Sub-Doppler mid-infrared spectroscopy of molecular ions," Chem. Phys. Lett. **551**, 1–6 (2012).
9. M. S. Taubman, T. L. Myers, B. D. Cannon, and R. M. Williams, "Stabilization, injection and control of quantum cascade lasers, and their application to chemical sensing in the infrared," Spectrochim. Acta A Mol. Biomol. Spectrosc. **60**(14), 3457–3468 (2004).
10. P. Ehlers, A. C. Johansson, I. Silander, A. Foltynowicz, and O. Axner, "Use of etalon-immune distances to reduce the influence of background signals in frequency-modulation spectroscopy and noise-immune cavity-enhanced optical heterodyne molecular spectroscopy," J. Opt. Soc. Am. B **31**(12), 2938–2945 (2014).
11. R. Drever, J. L. Hall, F. Kowalski, J. Hough, G. Ford, A. Munley, and H. Ward, "Laser phase and frequency stabilization using an optical resonator," Appl. Phys. B **31**(2), 97–105 (1983).
12. D. M. DeCain, P. C. Hobbs, and K. R. Pope, "Optical interferometer measurement apparatus and method," (Google Patents, 1999).
13. P. C. D. Hobbs, "Noise cancelling circuitry for optical systems with signal dividing and combining means" (Google Patents, 1992).
14. R. G. DeVoe, C. Fabre, K. Jungmann, J. Hoffnagle, and R. G. Brewer, "Precision optical-frequency-difference measurements," Phys. Rev. A **37**(5), 1802–1805 (1988).
15. A. Foltynowicz, F. M. Schmidt, W. Ma, and O. Axner, "Noise-immune cavity-enhanced optical heterodyne molecular spectroscopy: Current status and future potential," Appl. Phys. B **92**(3), 313–326 (2008).
16. E. J. Moyer, D. S. Sayres, G. S. Engel, J. M. S. Clair, F. N. Keutsch, N. T. Allen, J. H. Kroll, and J. G. Anderson, "Design considerations in high-sensitivity off-axis integrated cavity output spectroscopy," Appl. Phys. B **92**, 467–474 (2008).

#231015 - $15.00 USD Received 17 Dec 2014; revised 27 Jan 2015; accepted 27 Jan 2015; published 27 Feb 2015

17. D. D. Arslanov, M. P. Castro, N. A. Creemers, A. H. Neerincx, M. Spunei, J. Mandon, S. M. Cristescu, P. Merkus, and F. J. Harren, "Optical parametric oscillator-based photoacoustic detection of hydrogen cyanide for biomedical applications," J. Biomed. Opt. **18**(10), 107002 (2013).
18. O. Axner, P. Ehlers, T. Hausmaninger, I. Silander, and W. Ma, "Noise-immune cavity-enhanced analytical atomic spectrometry-NICE-AAS-A technique for detection of elements down to zeptogram amounts," Spectrochim. Acta, B At. Spectrosc. **100**, 211–235 (2014).
19. P. Ehlers, I. Silander, J. Wang, A. Foltynowicz, and O. Axner, "Fiber-laser-based noise-immune cavity-enhanced optical heterodyne molecular spectrometry incorporating an optical circulator," Opt. Lett. **39**(2), 279–282 (2014).

1. Introduction

Noise-immune cavity-enhanced optical heterodyne molecular spectroscopy (NICE-OHMS) is a laser-based spectroscopic detection method that comprises frequency modulation spectroscopy (FMS) and cavity enhancement, both sensitive spectroscopic techniques, to achieve exceptionally high sensitivities for the detection of molecular gases. FMS is an optical heterodyne technique that uses frequency modulation (FM) of laser light to produce sidebands on the laser frequency [1]. This modulation reduces the effect of 1/f-noise for sufficiently high modulation frequency and allows for the phase-sensitive detection of spectral features. With cavity-enhanced spectroscopy, the molecular gas is enclosed in a high finesse optical cavity to effectively increase the optical absorption path length. NICE-OHMS combines these two techniques by locking the laser frequency to a longitudinal mode transmission peak of the optical cavity; an additional modulation frequency is introduced that exactly matches the free spectral range (FSR) of the cavity. In this way, the transmitted FM triplet is kept balanced, because the three cavity modes interact with the three components of the triplet at exactly the same way. Therefore, the synchronous detection of the transmission signal at the FSR frequency is immune to the frequency-amplitude conversion noise between the incident laser and the cavity modes. NICE-OHMS has a very high sensitivity, because it combines FM with cavity enhanced absorption methods, where the FM signal is enhanced by a factor of $2F/\pi$, with F the cavity finesse. The technique was originally developed in the 1990s by Ye et al. [2] for frequency standard applications based on a narrow linewidth Nd:YAG laser, achieving a minimum detectable absorption sensitivity (NEAS) of 1 x 10^{-14} cm^{-1} $Hz^{-1/2}$ in 1 s averaging with a finesse of 10^5. Continuing this research, the technique has been implemented with various other lasers like fiber [3] or external cavity diode lasers (ECDL) [4–6]. The latter have a broader linewidth than Nd:YAG and fiber lasers, but possess the advantage of compactness and tunability over a wide wavelength range, making them ideal for molecular absorption applications in the near-IR. For example, Bell et al. detected CH_4 using an ECDL, achieving a NEAS of 4 x 10^{-11} cm^{-1} $Hz^{-1/2}$ with a finesse of 2600 [6]. The future potential for NICE-OHMS applications, however, resides in the realization of laser-based spectrometers operating in the molecular fingerprint region in the mid-IR. Recently, various mid-IR coherent light sources have been combined with NICE-OHMS, e.g. difference frequency generation [7], optical parametrical oscillators [8] or quantum cascade lasers [9]. For most of these approaches, the optical field gets modulated via an electro-optical modulator (EOM). Furthermore, most RF components for laser frequency stabilization, FSR matching and signal acquisition have to be matched to the specifics of the setup, which increases the complexity of the system. The use of EOMs or current modulation produces residual amplitude modulation (RAM) that can be reduced by electronic or optical means [1]. RAM is generally seen as a slow variation in the background, which limits the signal-to-noise ratio of the NICE-OHMS signals. This places great constrains on the perfection of alignment of an EOM to avoid RAM.

Additionally, in the mid-IR region, the use of EOMs becomes extremely costly. For further advancement of NICE-OHMS into the mid-IR and greater attractiveness for applications, a more straightforward approach and more user friendliness is essential. In this paper, we present a NICE-OHMS setup in the near-IR implementing commercially available locking tools using current modulation of the laser field for all modulations. We chose to work initially in the near-IR due to the better quality of the sources and detectors to ease the transition to the mid-IR. We assess the performance of the system using an ECDL for

#231015 - $15.00 USD Received 17 Dec 2014; revised 27 Jan 2015; accepted 27 Jan 2015; published 27 Feb 2015

Doppler-broadened absorption spectroscopy of methane, acetylene and hydrogen cyanide (HCN). Additionally, we studied the dynamics of the HCN production in sweet almonds to verify the applicability and sensitivity of the NICE-OHMS apparatus.

2. Experimental setup

For NICE-OHMS we apply two stages of FM to the laser light, which are demodulated sequentially. The first modulation ensures the lock of the laser to a single transmission peak of the cavity, while the second is at the cavity FSR to guarantee noise immunity. In this section, we describe the setup employing those two modulations to generate the NICE-OHMS signal.

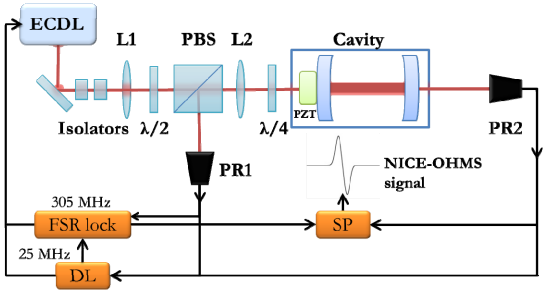

Fig. 1. Schematic of the NICE-OHMS setup employing solely current modulation. ECDL: External Cavity Diode Laser; PBS: Polarizing beam splitter; PZT: Ring piezoelectric transducer; λ/2 and λ/4: Half wave and quarter wave plate; PR1 and PR2: Photoreceivers 1 and 2; DL: Toptica Digilock; SP: Signal processor, L1 and L2: mode-matching lenses.

The experimental set-up is shown in Fig. 1. The external cavity diode laser (ECDL, DL pro, Toptica, Germany) used for the stabilization and spectroscopic experiments has a linewidth of 60 kHz < 5 μs), is tunable between 1510 – 1630 nm (power 50 mW), and possesses two current modulation inputs. In the optical path between the ECDL and the optical cavity two optical isolators (IO-4-1650-VLP, Thorlabs) are placed, passing through a half-wave plate (λ/2), a quarter-wave plate (λ/4) and a polarizing beam splitter (PBS) for optimizing the polarization and separate the reflection signal from the incoming beam. The optical isolators each provide 30 dB of isolation, protecting the ECDL from optical feedback from the cavity, which causes instabilities in the laser's frequency. The beam is mode-matched to the TEM_{00} mode of the cavity with two focusing lenses. Most optical elements are placed at etalon-free distances (integer multiples of the FSR) to couple a maximum of 65% of 0.5 mW incident power into the cavity [10]. The optical cavity is placed inside a vacuum chamber, which consists of an invar tube and two CaF windows mounted under an angle (25°) to minimize reflections. This configuration is chosen to avoid the influence of pressure changes on the optical cavity. The optical cavity is formed by two high reflectivity mirrors (25 mm diameter, radius of curvature r = 1 m, reflectivity R = 99.8% at 1.6 μm) with a length of 49.2 cm, resulting in a cavity FSR of 304.9 MHz. One mirror is mounted on a piezoelectric ring actuator (Physik Instrumente P-025.40H) and is used for scanning the cavity length over a maximum of 6 GHz with a scanning rate of 5 Hz. Two photoreceivers (HCA-S-400M-IN-FS, bandwidth 400 MHz, Femto) monitor signals in reflection and transmission; they are used for laser frequency stabilization and molecular spectroscopy. The wavelength was monitored with a wavelength meter (Bristol Instruments 621A).

We measure three different gases covering the tuning range of the ECDL (CH_4 at 6132.3 cm^{-1}, C_2H_2 at 6578.5 cm^{-1} and HCN at 6541.7 cm^{-1}) without re-aligning or adapting the optical components. The cavity is evacuated to 10^{-3} mbar before molecular gas is introduced via a mass flow controller (Brooks Instruments). To analyze the gas inside the cavity, the transmission detector output is sent to a data acquisition card (NI-6239, National Instruments), averaging five individual spectra (870 points) in an acquisition time of 1 s for post processing in Matlab.

#231015 - $15.00 USD Received 17 Dec 2014; revised 27 Jan 2015; accepted 27 Jan 2015; published 27 Feb 2015

Two servo-locking systems exist in our NICE-OHMS setup. The first is used to lock the laser to a cavity mode and the second to match the frequency of the FSR. For this, our setup employs two modulation frequencies at 25 and 305 MHz, both added to the current of the laser via a Bias-T on one of the current inputs. The laser frequency is locked to a longitudinal mode of the cavity by the Pound-Drever-Hall (PDH) method (β = 0.12) [11]. Within this method, the reflected light from the first cavity mirror is directed via the PBS and a λ/4-plate to the photodiode. The resulting signal is demodulated to generate an error signal, which is fed to a noise canceler based on the patent of DeCain et al. [12, 13] and a commercial Toptica Digilock in order to maintain the laser frequency at the peak of the cavity resonance. The Digilock requires minimal setting adjustment and the automated locking procedure is straightforward. Evaluation of the transfer functions of the laser and the locking servo occurs via internal routines. The servo loop has a bandwidth of 1 MHz and allows for fast feedback to the laser current via a second current input, whereas low frequency signals are fed back to the laser piezo to allow a wide tuning range. Once locked with sufficient bandwidth, the cavity can be swept over 6 GHz, while the laser is following.

The second modulation frequency, employed at υ_{FSR} for noise immunity, is injected into the current at 305 MHz. The noise-immune aspect of NICE-OHMS requires a good match between the modulation frequency and υ_{FSR}. For this, we use the locking scheme by DeVoe and Brewer [14]. A fraction of the cavity reflection signal from is split off and demodulated at 280 MHz (the difference of υ_{FSR} and υ_{PDH}) to produce the error signal. A PID controller with a 300 kHz bandwidth then adjusts the frequency of oscillators to match the FSR of the cavity. To produce the NICE-OHMS signal, the transmission signal is high-pass filtered (Mini-Circuits SHP-175) and then demodulated at υ_{FSR} with a double balance mixer (Mini-Circuits ZLW-1). This signal is passed through an 80 Hz low-pass filter (Mini-Circuits PLP-10.7) and recorded via the data acquisition card. Changing the demodulation phase allows either the absorption or dispersion FMS signal to be acquired. MATLAB is used to fit the measured NICE-OHMS lineshape function [15].

3. Results and discussion

To analyze the performance of the spectrometer over a broad wavelength range and to demonstrate the capability of the current modulation approach, we measured molecular transitions of methane, acetylene and HCN. Figure 2 shows a Doppler-broadened Nice-OHMS signal for both the dispersion (Fig. 2(a)) and the absorption case (Fig. 2(b)), at a concentration of 200 ppbv methane in N_2 at a wavelength of 6132.3 cm^{-1} (pressure 3 mbar, scanning rate 5 Hz over 1.5 GHz). At this pressure, no sub-Doppler features are visible in the spectrum. With a modulation index of β = 0.54, the RAM in the system amounted to ~6%.

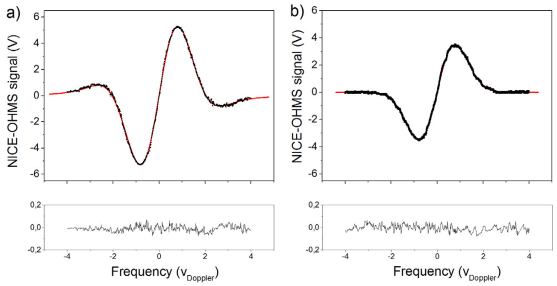

Fig. 2. NICE-OHMS signal of 200 ppbv methane at 6123.3 cm^{-1} for dispersion (panel a) and absorption (panel b) as a function of Doppler frequency (473 MHz). Black dots represent measurement points, with a fit in red. Residuals of each plot are given below.

A similar approach is used to acquire absorption NICE-OHMS signals for 100 ppbv C_2H_2 at 6578.5 cm^{-1} and 200 ppbv HCN at 6541.7 cm^{-1} at 3 mbar (Fig. 3(b) and 3(c)) within 1 s averaging time. The resulting absorption signal for acetylene is the strongest of all three compounds. Due to wide wavelength coverage, the optical isolators are not able to suppress

#231015 - $15.00 USD Received 17 Dec 2014; revised 27 Jan 2015; accepted 27 Jan 2015; published 27 Feb 2015

etalon effects strongly, which results in the intensity variations clearly seen in the spectra of acetylene and HCN.

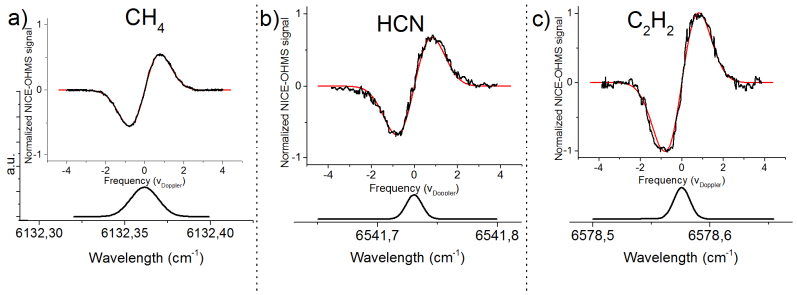

Fig. 3. Measured (black line) and simulated (red line) NICE-OHMS absorption signals at 3 mbar from (a) 200 ppbv of methane, (b) 200 ppbv of HCN and (c) 100 ppbv of acetylene together with simulated absorption peaks below the corresponding graph.

We calculate the minimum noise equivalent absorption sensitivity (NEAS) per spectral element of the setup for all three compounds based on the expression given by Eq. (16) in Moyer et al. [16]

$$NEAS = \left(\frac{\Delta I}{I_0}\right)_{\min} \frac{\sqrt{nT}}{L_{\text{eff}}\sqrt{N_p}} \tag{1}$$

where $(\Delta I/I_0)_{min}$ is ratio of the noise on the baseline of the absorption signal and the maximum transmission in the absence of an absorber, L_{eff} is the effective optical path length, n is the number of scans integrated, T the acquisition time per scan and N_p the number of data points per spectrum. Our best achieved NEAS has a value of 4.1 x 10^{-10} cm^{-1} $Hz^{-1/2}$. The theoretical shot-noise limited NEAS of the NICE-OHMS setup is calculated based on Eq. (8) of Foltynowicz et al. [15] and gives 3.8 x 10^{-12} cm^{-1} $Hz^{-1/2}$. Thus, the sensitivity reported here is a factor 100 above the shot-noise limit. The detection limits can be calculated by dividing the concentration of the gas under study by the signal-to-noise ratio (SNR), which gives a value of 0.93 ppbv for methane with a SNR of 215. The SNR is calculated by dividing half the peak-to-peak value of the NICE-OHMS signal by the root-mean-square of the data. For acetylene and HCN the detection limit deteriorates a factor 2 and 3.5, respectively. This is a direct result from the increased noise on the NICE-OHMS signal.

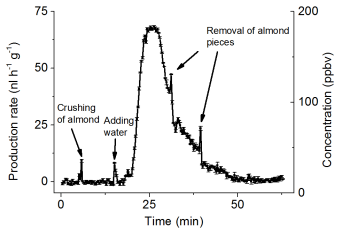

Fig. 4. Dynamics of HCN production in sweet almonds over 75 min. The values are means of the production rate of three repeated experiments. The almonds are crushed after 15 min and start to produce HCN with a maximum of 68 µl h^{-1} g^{-1} 10 min after crushing. In intervals of 10 min, half the almond pieces are removed. The production rate of the remaining almond pieces reaches the background level after 60 min.

Having shown the capability of the system, we apply the NICE-OHMS system to the detection of HCN emission from sweet almonds. Figure 4 shows the dynamics of the HCN production over time. The data is averaged over 100 scans every 20 s and the experiment is repeated three times. Initially, the almonds are flushed at 1 l/h with N_2 at room temperature in a glass cuvette for 5 min, after which they are crushed. The peaks in Fig. 4 indicate a

#231015 - $15.00 USD Received 17 Dec 2014; revised 27 Jan 2015; accepted 27 Jan 2015; published 27 Feb 2015

disturbance in the system due to the opening of the cuvette. At first no HCN is present, while adding water (1 ml after 15 min) fuels the HCN production. After 2 min the HCN production rises to 68 µl h^{-1} g^{-1} within 7 min, after which the HCN production decreases gradually. At 30 min and 39 min, half of the almond pieces are removed from the cuvette, lowering the production rate by a factor of ~2. From 40 min on, the HCN values fall off exponentially until the production ceases completely at 60 min. For validation the data is compared to previously taken measurements with almonds taken with an OPO-based photoacoustic setup described elsewhere [17].

The two common noise sources of NICE-OHMS setups are also present in our system: etalon effects created by reflections between optical surfaces, and RAM generated by the conversion from FM to AM during the current modulation. The former can be minimized by placing optical elements at etalon immune distances and adding anti-reflection coating to surfaces. Additionally, optical isolators in front of the laser are important to suppress any feedback into the laser, which greatly disturbs the stability of the laser's frequency. For the molecular transitions we studied, RAM is mostly removed by background subtraction and optimization of the modulation frequency [9, 12]. In general, using the whole tuning range makes the system less sensitive as compared to a situation where the system is be optimized for a specific wavelength. This is clearly seen in the increased noise after changing the laser wavelength by ~400 cm^{-1}. In addition, the use of a generic, commercial locking device yields only average lock quality and performs less than a specifically matched one. For example, the Digilock contains only a single stage PID controller, whereas a double integrator was needed to achieve sensitivities of ~10^{-12} cm^{-1} $Hz^{-1/2}$ [18, 19]. Using a cavity finesse in the order of 10^4 or higher would be very difficult to lock with the current commercially available devices as the lock needs to be much more stable to keep the laser in the narrow cavity mode. In addition, from the above measurements across the tuning range of the laser, it becomes clear that the use of a commercial servo lock has its limitations with respect to locking bandwidth and efficiency, if the transfer functions of the laser and the cavity change when tuning the laser wavelength. Nonetheless, employing current modulation and commercial devices reduces the time-consuming procedure of precise EOM alignment and fabrication of advanced home-made electronics. In spite of the variation in sensitivity across the tuning range, the system presented here has the ability to apply NICE-OHMS to various molecular gases, achieving only slightly lower sensitivities compared to other ECDL-based systems of ~10^{-11} cm^{-1} $Hz^{-1/2}$ with higher cavity finesses and wavelength modulation [4, 6]. The system can be enhanced by the use of a higher cavity finesse and more advanced servo circuitry. However, the key issue here is not to strive for a better sensitivity or stability, but to a simplification, such that this method can be employed efficiently with mid infrared lasers systems. Therefore, in the near future we will evaluate the implementation of current modulated NICE-OHMS with a broadband laser in the mid-IR.

4. Conclusion

In summary, we have presented a simplified approach to implement NICE-OHMS using current modulation and commercial devices. A full description of our NICE-OHMS apparatus is given, and measurements of methane, acetylene and hydrogen cyanide at sub-ppbv levels are shown, resulting in noise equivalent absorption sensitivities of 4.1 x 10^{-10} cm^{-1} $Hz^{-1/2}$. The dynamics of the HCN production in sweet almonds is used to show the system's stability and applicability to sensitive trace gas detection. We aim to apply this current modulation approach in the mid-IR region for the sensitive detection of broadband absorption molecules.

Acknowledgments

This work was supported by the Foundation for Fundamental Research on Matter under contract N0304M and the European Regional Development Fund, province of Gelderland, GO-EFRO project (no. 2009-010034).

#231015 - $15.00 USD Received 17 Dec 2014; revised 27 Jan 2015; accepted 27 Jan 2015; published 27 Feb 2015